Guided elastic waves along a rod defect of a two-dimensional phononic crystal

A. Khelif, M. Wilm, V. Laude, and S. Ballandras
Institut FEMTO-ST, Département LPMO, CNRS UMR 6174, 32 avenue de I'Observatoire, 25044 Besançon cedex, France

B. Djafari-Rouhani
Laboratoire de Dynamique et Structures des Matériaux Moléculaires, CNRS UMR 8024, Université de Lille I, 59655 Villeneuve d'Ascq cedex, France
(Received 19 November 2003; published 11 June 2004)

It was shown that elastic waves propagating out-of-plane in a two-dimensional phononic crystal can experience full-band-gaps for nonzero values of the wave-vector component parallel to the rods. By further inserting a rod defect, it is demonstrated that modes propagating along the rod defect can be localized within the band-gaps of the phononic crystal. Such waveguide modes are exhibited for a tungsten/epoxy composite containing an aluminum nitride rod as the rod defect. It is expected that guided modes of such a structure can be excited and detected electrically owing to the piezoelectric effect.

DOI: 10.1103/PhysRevE.69.067601 PACS number(s): 43.20.+g, 43.40.+s, 46.40.Cd, 63.20.−e

The propagation of classical waves in periodic structures is receiving increasing attention as a generic procedure for obtaining innovative or enhanced functions in passive components dedicated to signal processing. Most studies have been focused on photonic crystals, for which the appearance of frequency gaps for the propagation of electromagnetic waves has been demonstrated both theoretically and experimentally, and which are used for the achievement of new optical devices. In parallel, the propagation of elastic and acoustic waves in periodic structures made of materials with different elastic properties, also called phononic crystals, is receiving a growing interest. For instance, in the case of elastic waveguides, bulk localized states have been predicted [1,2] while surface states as well as localization phenomena have been calculated and observed in linear and point defects [3]. Localized states have also been investigated in relation to planar defects [4].

In a recent work [5], we investigated the out-of-plane propagation of elastic waves in a two-dimensional phononic band-gap material composed of quartz rods embedded in an epoxy matrix. Band-gaps for nonzero values of the wave-vector component parallel to the rods were shown to exist. It is essential for applications of a such a two-dimensional periodic structure, that displays an absolute band-gap in its phononic band structure for in-plane propagation, to know the extent to which acoustic waves can propagate out of plane while an in-plane absolute band-gap can still be seen in the corresponding band structure. Also, the possibility of guiding waves propagating perpendicularly to the plane of the structure is revealed by such an analysis. The presence of a piezoelectric material offers the possibility of exciting and detecting waves electrically in the structure using the piezoelectric effect. Interestingly, the frequencies of elastic modes are in general only slightly affected by piezoelectric coupling, that is less than 1% even for rather strong piezoelectrics. The occurrence of frequency gaps and localized modes is then very slightly modified by piezoelectricity. In this paper, we investigate theoretically the propagation of guided elastic waves in a two-dimensional periodic structure, that consists of an array of infinitely long parallel square-section rods of tungsten embedded in an epoxy matrix. The advantage of a metal such as tungsten with respect to a material such as quartz lies in the much higher impedance ratio with epoxy, which results in the formation of full-band-gaps with lower filling fractions, or of larger band-gaps for the same filling fraction. The intersections of the rods' axes with the perpendicular plane form a two-dimensional Bravais lattice. To achieve out-of-plane propagation with a confinement in the (x,y) plane, we add a piezoelectric rod defect, in this case aluminum nitride (AlN), with the intent of breaking the periodicity and inducing localized modes in the band-gaps. The AlN C-axis is directed along the z axis since this configuration is the most favorable for the excitation of compressional waves. Numerical calculations are performed using a plane-wave-expansion (PWE) method, which was originally developed for 1-3 connectivity piezoelectric composites [6] and further adapted to anisotropic solid-solid phononic band-gap materials [5].

Figure 1(a) displays the cross-section of the phononic crystal considered in this work. This phononic crystal is composed of tungsten rods in an epoxy matrix. The tungsten inclusions are arranged periodically on a square lattice and are assumed to have a square cross-section so that the filling

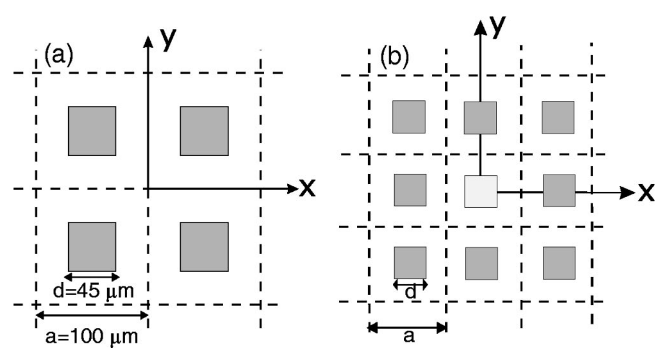

FIG. 1. (a) Cross-section of a bi-periodic solid-solid phononic band-gap material, consisting of tungsten rods in epoxy. (b) Cross-section of a super-cell solid-solid phononic band-gap material, consisting of AlN rod defect in tungsten/epoxy structure.

 ©2004 The American Physical Society

TABLE I. Mechanical constants of aluminum nitride (AlN), tungsten (W) and epoxy. Only independent constants are given for each material.

Material	Mass density (kg/m^3)	Elastic constants (10^{10} N/m^2)					Piezoelectric constants (C/m^2)			Dielectric constants (10^{-11} F/m)	
	ρ	c_{11}	c_{12}	c_{13}	c_{33}	c_{44}	e_{15}	e_{31}	e_{33}	ϵ_{11}^S	ϵ_{33}^S
AlN	3260	34.5	12.5	12	39.5	11.8	−0.48	−0.58	1.55	8	9.5
W	19300	50	…	…	…	15.13	…	…	…	…	…
Epoxy	1142	0.7537	…	…	…	0.1482	…	…	…	3.8	…

fraction $(d/a)^2$ is 0.20. For instance, the width of the inclusions $d=45$ μm for a lattice parameter $a=100$ μm. This choice of materials provides a very high scattering contrast since the ratio between the longitudinal acoustic impedances of tungsten and epoxy is around 35. Table I displays the material constants used in the computations. 6×6 Fourier and Bloch-Floquet harmonics are used for computations of the perfect phononic crystal band structure. Let us notice that for off-plane propagation considered in this paper the three components of the displacement field remain coupled together. A very accurate convergence of the results, using the PWE method, will require the use of more Fourier components in the expansion of the parameters and the displacement field. However, we have chosen to limit this number for the following reason. In studying localized modes associated with the rod defects, we shall need to introduce a super-cell much larger than the unit cell of the phononic crystal. Accordingly, the number of the reciprocal wave vectors needed to obtain the same convergence properties as for the perfect phononic crystal will considerably increase. Therefore, in choosing the number of reciprocal wave vectors taken into account, our aim is to obtain a good physical description of the band structures within the limitation related to computation possibilities.

Figure 2 shows the band structures in the (k_x,k_y) plane projected onto the reduced-frequency normalized-wave-vector plane. The reduced-frequency is defined as fa, where f is the frequency, while the normalized-wave-vector $\gamma_z=k_z a/2\pi$. The out-of-plane wave-vector component k_z corresponds to the propagation constant along the axis of the tungsten rods and is normalized with respect to the center-to-center distance a between the two nearest tungsten rods. Figure 2 reveals several band-gaps that appear in white. Several absolute band-gaps for nonzero out-of-plane wave-vectors are visible, although the filling fraction is quite small (20%). No propagation and no vibration are allowed in these regions. For $\gamma_z=0$, two band-gaps appear in the (k_x,k_y) plane that are labeled (b) and (c). For these gaps, the ratios of the bandwidth to the midgap equal 43% and 19%, respectively. When γ_z increases, the widths of band-gaps (b) and (c) decrease and vanish when $\gamma_z\simeq 0.29$. At the same time, other band-gaps labeled (d), (e), (f), (g) and (h) appear. The frequency width and the extension of the band-gaps as a function of γ_z are different. The width of the low-frequency band-gap, labeled (a) in Fig. 2, is seen to increase quasi-monotonically from zero with increasing γ_z. In fact, when $\gamma_z\neq 0$ there is a minimum frequency below which no extended solutions exist. This is because the slowest wave in the structure is the bulk-epoxy transverse mode, irrespective of the values of k_x and k_y. Thus, a band-gap below the first band opens up in the phononic band structure for nonzero γ_z, whose width increases as γ_z increases.

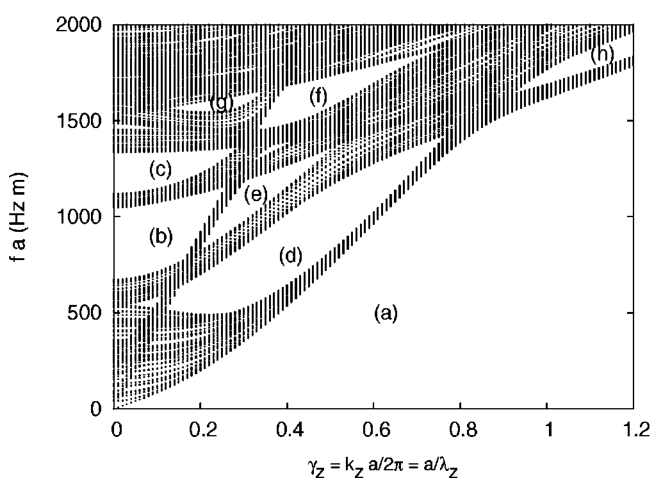

FIG. 2. Projection of the phononic band structures in the (k_x,k_y) plane onto the (k_z,f) plane, for the tungsten-epoxy phononic crystal. Delimited white regions indicate absolute stop-bands in the (k_x,k_y) plane.

In order to achieve waveguiding along the rods, we break the periodicity of the structure by introducing a defect. This is produced by replacing one tungsten rod by one aluminum nitride (AlN) rod, as depicted in Fig. 1(b). The width of the square section of the AlN rod is the same as for tungsten rods, i.e., 45 μm for a period of 100 μm. The longitudinal acoustic impedance of AlN is ten times larger than that of epoxy, although it is three times less than that of tungsten. For practical computations, a super-cell is defined so that the AlN/tungsten/epoxy structure can still be investigated with the PWE method. The super-cell is a 3×3 tungsten-rod array with the central rod replaced by an AlN rod, as depicted in Fig. 1(b). Since the super-cell is three times larger than the elementary cell, 18×18 Fourier and Bloch-Floquet harmonics are used for computations with the defective phononic crystal, in order to retain the same convergence properties.

In order to investigate the changes induced by the presence of the AlN rod defect, Fig. 3 displays the dispersion diagram for modes that propagate inside the structure with a propagation constant $\gamma_z=0.1$. Four band-gaps are apparent. From low to high frequencies, the first, third and fourth

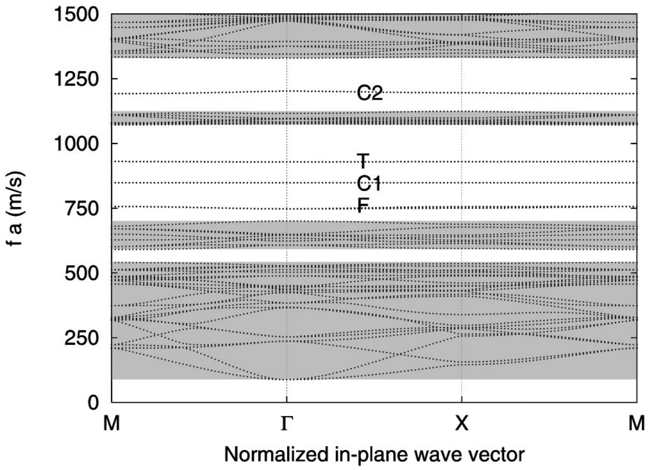

FIG. 3. The phononic band structures in the (k_x, k_y) plane along the M-Γ-X-M path for $\gamma_z = 0.1$, for the tungsten/epoxy/AlN structure. Defect modes appear in two band-gap regions.

band-gaps are labeled (a), (b) and (c), respectively in Fig. 2. When introducing the defect rod, four flat branches — labeled F, C1, T, and C2 — appear in the band-gap regions. Three of them appear in the third band-gap and one in the fourth. Whatever the in-plane wave-vector, there is no dispersion for these defect modes, i.e., they are localized in the (x,y) plane around the defect region with a transverse group velocity $(d\omega/dk)$ equal to zero. This is a clear indication that guided modes exist for frequencies inside the band-gaps. In order to illustrate the confinement of defect modes, the eigenvectors for all flat branches are plotted in Figs. 4 and 5. Among these maps, the F and T modes depicted in Fig. 4 have mostly an in-plane polarization. Indeed, mode F depicted in Fig. 4(a) is the fundamental flexural mode of the

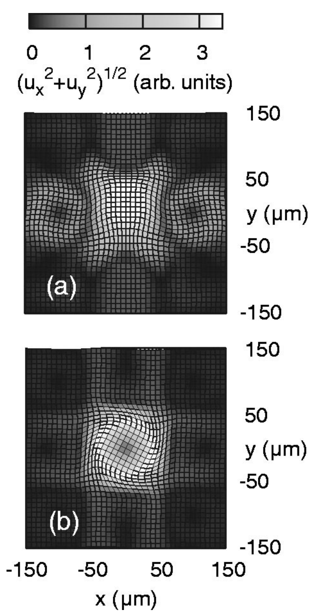

FIG. 4. Relative magnitude of in-plane displacements for (a) the flexural mode, F, with $fa = 751.9$ m/s and (b) the torsional mode, T, with $fa = 929.0$ m/s for the tungsten/epoxy/AlN structure. $\gamma_z = 0.1$ for these computations.

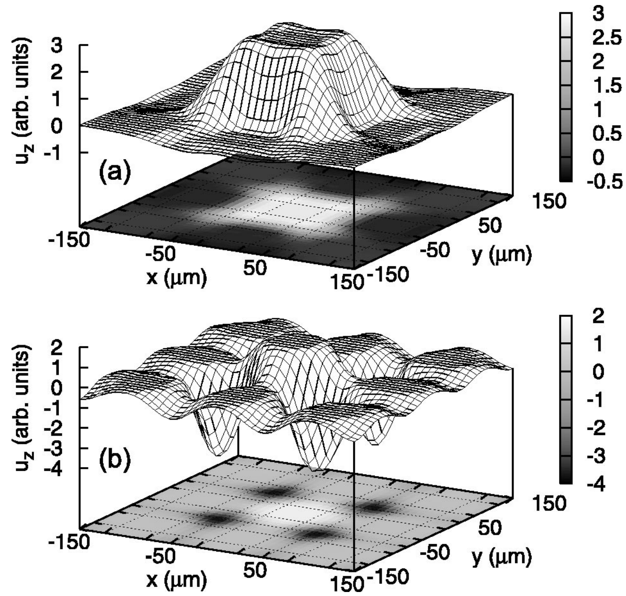

FIG. 5. Relative magnitude of out-plane displacements of (a) the compression mode, C1, with $fa = 848.0$ m/s and (b) the compression mode, C2, with $fa = 1198.4$ m/s for the tungsten/epoxy/AlN structure. $\gamma_z = 0.1$ for these computations.

rod defect with only components u_x and u_y in the (x,y) plane. This mode is in fact degenerate because of the in-plane isotropy of the structure. Similarly, mode T depicted in Fig. 4(b) is a torsional mode with components u_x and u_y, that is localized around the rod defect. Modes C1 and C2 are depicted in Fig. 5. These modes are of the longitudinal or compressional type, with mostly a u_z component, and they are localized inside and in the vicinity of the rod defect. Mode C1, depicted in Fig. 5(a), is well confined inside and around the AlN rod. Mode C2, depicted in Fig. 5(b), has a more complex structure as the displacements of the AlN rod and of the epoxy interstice are in opposite phase.

It is remarkable that the modes that have been found are exactly of the same types as those found in classical elastic waveguides [7], i.e. we identified flexural, torsional and compressional modes. In classical elastic waveguides, the boundary conditions are responsible for the apparition of a discrete number of guided modes. In the present case, the phononic crystal surrounding the defect rod plays a similar role for frequency intervals within which an absolute band-gap exists.

The four guided modes described above are spatially localized in the defect region in the (x,y) plane, but they are propagative in the z direction. Figure 6 shows the band structures in the (k_x, k_y) plane projected onto the reduced-frequency normalized-wave-vector plane, for the tungsten/epoxy/AlN structure. These band structures are to be compared with those of perfect phononic crystal, i.e., the tungsten/epoxy structure, displayed in Fig. 2. The white regions again indicate absolute band-gaps in the (k_x, k_y) plane. It can be noticed that the band-gaps obtained with the supercell are almost identical to those obtained with the elementary cell. This demonstrates that the band-gap properties of the phononic crystal are not significantly perturbed by the

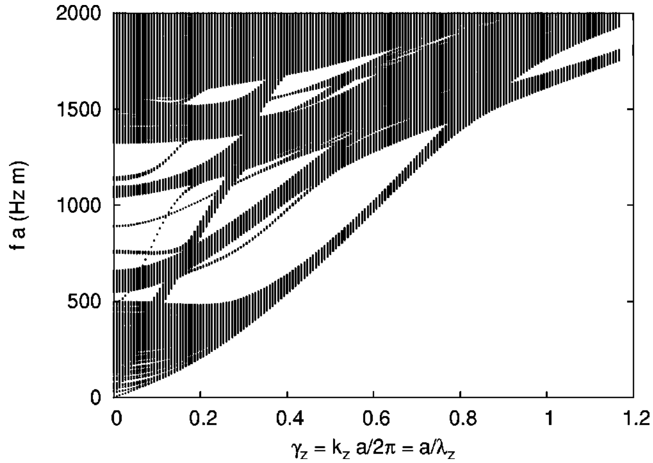

FIG. 6. Projection of the phononic band structures in the (k_x, k_y) plane onto the (k_z, f) plane, for the tungsten/epoxy/AlN structure. Delimited white regions indicate absolute stop-bands in the (k_x, k_y) plane. Defect modes appear in these regions.

inclusion of the periodic defect. The branches that now appear inside the band-gaps are those of defect modes and are representative of their dispersion as a function of the z component of the wave-vector. It can be seen that the phononic crystal with a rod defect possesses several guided modes that can exist within the different band-gaps. If γ_z is held constant, then these modes give rise to flat branches in the (k_x, k_y) plane as in Fig. 3. Consequently, their group velocities are zero in the transverse plane and they are constrained to propagate along the rod axis. Let us also notice that when γ_z decreases from 0.5 to 0, the frequency of the flexural mode in Fig. 3 decreases as well and finally the corresponding dispersion curve merges with a bulk band. At the same time, the other modes (T, C1 and C2) depicted in Fig. 3 change only slightly and the corresponding eigenvectors remain almost unchanged with respect to those shown in Figs. 4 and 5. In practice, to excite a guided mode at a given frequency, the piezoelectric defect rod should be submitted to an applied electric field. Since the defect mode is situated in an absolute band–gap for in-plane propagation, the excitation should remain mainly localized in the vicinity of the defect rod. Nevertheless, it should be mentioned that the phononic crystal does not display any omnidirectional gap for propagation in the three-dimensional space, which means that, for a given frequency, bulk modes of the crystal coexist simultaneously with the guided mode.

In summary, we have computed the phononic band structure of an infinite square array of parallel tungsten rods embedded in an epoxy matrix, forming a two-dimensional phononic crystal. For nonzero values of k_z, the phononic crystal possesses absolute band-gaps in the plane perpendicular to the rods, i.e., for all polarizations of elastic waves propagating in the plane of the structure. We have established the occurrence of defect modes by replacing one tungsten rod by an aluminum nitride rod in the tungsten/epoxy composite. These modes can be found inside the band-gaps, with their vibration being localized in the vicinity of the defect sites. They are therefore capable of propagating energy along the rod defect. As a consequence, this study predicts the possibility of achieving solid-solid phononic fibers supporting guided elastic waves along their axis.

[1] A. Khelif, B. Djafari-Rouhani, J. O. Vasseur, P. A. Deymier, P. Lambin, and L. Dobrzynski, Phys. Rev. B **65**, 174308 (2002).
[2] M. Kafesaki, M. M. Sigalas, and N. Garcia, Phys. Rev. Lett. **85**, 4044 (2000).
[3] M. Torres, F. R. Montero de Espinosa, D. García-Pablos, and N. García, Phys. Rev. Lett. **82**, 3054 (1999).
[4] I. Psarobas, N. Stefanou, and A. Modinis, Phys. Rev. B **62**, 5536 (2000).
[5] M. Wilm, A. Khelif, S. Ballandras, V. Laude, and B. Djafari-Rouhani, Phys. Rev. E **67**, 065602(R) (2003).
[6] M. Wilm, S. Ballandras, V. Laude, and T. Pastureaud, J. Acoust. Soc. Am. **112**, 943 (2002).
[7] D. Royer and H. Dieulesaint, *Elastic Waves in Solids* (Springer, New York, 1999).